07912-4-P

THE UNIVERSITY OF MICHIGAN

COLLEGE OF ENGINEERING
DEPARTMENT OF AEROSPACE ENGINEERING

Progress Report

Fluid Mechanics of Magnetically Balanced Arcs in Cross Flows

S. W. BOWEN

Administered through:

March 1968

OFFICE OF RESEARCH ADMINISTRATION • ANN ARBOR

Progress Report

FLUID MECHANICS OF MAGNETICALLY BALANCED ARCS IN CROSS FLOWS

S.W. Bowen

ORA Project 07912

March 1968

SUMMARY OF ACTIVITIES
(September 1, 1967 - February 29, 1968)

Work has continued on various aspects of the magnetically balanced air arc in supersonic flow.

The Ph.D. thesis of R. L. Harvey entitled, "An Experimental and Theoretical Investigation of Magnetically Balanced Arcs," has been satisfactorily accepted by the Graduate School.

Mach numbers between 2.5 and 3.5 at stagnation pressures between .35 and 1 atm were investigated with arc currents from 130 to 700 amperes. Magnesium tracer particles, injected into the arc near the upstream anode root and followed photographically along nearly the whole arc length, showed a longitudinal axial flow within the arc on the order of 10 m/sec while the free stream velocity was about 600 m/sec. These observations directly indicate the balanced positive column is impervious to the free stream.

Column drag coefficients and Nussult numbers were found to be of the same order as the corresponding values for heated solid cylinders.

A mathematical model based upon the analogy between the Lorentz force and buoyancy forces is used to show that an internal double vortex flow is generated even without the external free stream shearing forces. The maximum temperature peak is shifted forward as the dimensionless free stream velocity is increased.

L. M. Nicolai has continued with his studies concerning the affect of the significant parameters on the behavior of the convected arc. He has been able to categorize the arc power input as a function of the Lorentz convection parameter L_C. As $L_C \to 0$ (free burning arc) EI/ϕ is independent of L_C, for intermediate values of L_C, $EI/\phi \sim L_C$ and for large L_C, $EI/\phi \sim \sqrt{L_C}$. ϕ is the heat flux potential. A criteria indicating when L_C is "large" and when L_C is "intermediate" has been obtained.

Further, more sophisticated computer studies of the temperature distribution within the arc are in progress.

Some experimental studies made upon the high current, low pressure, free burning arc, show flat E vs I characteristics for $I > 100$ amp. These studies should enable greater understanding of the transition occurring between the free burning and convected arc, i.e. as L_C increases from zero. It is expected that these studies will be submitted as a NASA Contractors Report.

Appendix A contains a comprehensive discussion entitled, "Experimental Investigation of a Magnetically Balanced Arc in a Supersonic Cross Flow," by A. M. Kuethe, R. L. Harvey, and L. M. Nicolai.

EXPERIMENTAL INVESTIGATION OF A MAGNETICALLY

BALANCED ARC IN A SUPERSONIC CROSS FLOW

A. M. Kuethe
R. L. Harvey
L. M. Nicolai

SUMMARY

Experimental results on steady magnetically balanced arcs in supersonic external flows are presented and are analyzed, along with investigations elsewhere in subsonic flows, to determine the important similarity parameters. The studies indicate that the steady arc has a central core, impervious to the external flow, within which differential Lorentz forces generate a circulation analogous to that generated by gravity forces in a non-uniformly heated gas in a horizontal tube. The conservation equations indicate that a "Lorentz convection parameter," analogous to the Grashof number in free convection phenomena, an important similarity parameter over a significant range of arc variables. A "characteristic velocity" for the core circulation is indicated. The similarity parameters that provide the interpolation between the properties of subsonic and supersonic balanced arcs indicate approximations inherent in the conservation equations to provide a valid first order solution for the internal circulation.

1. INTRODUCTION

Our knowledge of even the gross aspects of mass, momentum, and energy transfer between an arc and an external stream depends today almost completely on empirical data. However, solutions to such practical problems as determination of the mass loss from a gaseous fission reactor, and the maximization of the acceleration in $\vec{J} \times \vec{B}$ or $\vec{E} \times \vec{B}$ accelerators will require detailed knowledge of fluid and plasma interactions such as occur at the boundary of a balanced arc. This paper identifies, through inference from the conservation equations and experimental data, some features of these mechanisms and the governing parameters.

The first instance of a steady arc balanced magnetically in a cross-flow of appreciable velocity was reported by Bond in 1962[1]. Subsequent investigations[2,3], in which fairly intense external magnetic fields were utilized to balance dc arcs in supersonic external flows, led to the determination of the gross properties of these arcs. One of these properties, a slant angle a few degrees greater than the Mach angle of the external flow was found to occur whenever the arc was steady; the cause of the slant is not known but Bond pointed out[2] that the degree of ionization within the arc will be near its maximum if the arc slants at the Mach angle. *

---

*Bond and Potello[4] have recently reported on experiments on arcs moving along heated electrodes under the influence of a uniform external magnetic field. They find very nearly the same slant angle to the relative flow as was found in the balanced arc tests, which were carried out in a supersonic tunnel with an external magnetic field that varied in the stream direction.

The experimental work presented here utilized the equipment described in Ref. 1-3 and extends the work toward the delineation of a model of the arc as a basis for calculating the fluid mechanical structure of the arc. The equipment provided the field configuration indicated in Fig. 1 in which the arc was initiated by an exploding wire between rail electrodes parallel to the external flow. The balance between the aerodynamic and the Lorentz forces was achieved by means of an external magnetic field oriented normal to the electric field and to the external flow direction.

The work of Roman[5] and Myers[6,7], shows that a steady magnetically balanced arc can be achieved when the arc is generated across a free jet at subsonic air speeds.* The arc was generated between coaxial pin electrodes and was normal to the flow, it was remarkably steady over a range of arc currents and jet speeds, so that traverses of velocity and enthalpy in the wake could be made.

These measurements at subsonic and at supersonic speeds provide a basis for examining the extent to which the fluid mechanical structure of the arc can be described by the equations of continuum mechanics of a conducting fluid. The experimental data are used to calculate the non-dimensional parameters indicated by the momentum and energy equations; the validity of the approximations made are inferred from the behavior of the parameters.

---

*This configuration will, in this report, be referred to as a "subsonic balanced arc" while that used by Bond and the present authors will be called a "supersonic balanced arc."

2

Some limited attempts have been made[8-11], to attack the problems of the balanced arc by solving the conservation equations for the entire flow field. Since the experiments indicate that the arc core is impervious to the external flow, the complete solution would comprise determination of the flow field, internal and external, for a plasma column whose dimensions are determined by the equilibrium conditions between the internal and external pressure fields. The solution is incomparably more difficult than that of determining the flow field around a solid body of fixed dimensions. For the arc, even if the cross-section shapes were known, the boundary conditions necessary for calculating the flow in the boundary layer and particularly near the flow separation point are unknown. One is accordingly forced to seek a model of the arc which will provide a framework for calculating arc properties under circumstances which can be checked by experiment.

The experimental results were used to evaluate the non-dimensional parameters that occur in the conservation equations (see Fig. 8 and 9). The functional relationships which emerge indicate there is a range of field properties over which the internal circulation can be determined to first order by means of solutions of the conservation equations for incompressible flow of a conducting fluid, neglecting radiation, nonequilibrium, Hall currents, and the effect of the current induced by the motion of the conducting fluid through the induced and applied magnetic force lines.

3

2. THE ARC COLUMN AS AN IMPERVIOUS CYLINDER

Axial flow along the arc, which is a sufficient condition that the external stream flows around, rather than through the arc, was observed earlier by the first two authors[12,13]; high speed motion pictures showed particles of the anode material moving along the arc from anode to cathode at speeds around 30 ft/sec. The picture was taken nearly head on and shows the arc extending from the anode (bottom) toward the cathode, then curling around it to form the cathode root about 120° from the point nearest the anode. This behavior probably comes about because the Lorentz force deflects the column until the current enters the cathode along a line parallel to the magnetic lines of force.

In the later work two simultaneous exposures were taken, one direct and one reflected, as shown diagrammatically in Fig. 2, so that approximate dimensions of the arc could be determined. High speed motion pictures were taken of magnesium particles which were drawn into the stream from a hollow anode. Figure 3 is a sequence of the simultaneous exposures tracing the motion of a vaporizing particle of magnesium; the first appearance of the particle is immediately behind the arc in frame 2. The succeeding frames indicate the motion of the particle along a path inclined upward and downstream, indicating that the air speed in the wake is extremely low. An interesting feature in frame 2 is that in the nearly head-on view the particle is photographed through the arc, indicating that the arc is not opaque to at least some of the magnesium radiation.

4

The measured speeds of particles along the arc give a lower bound for the axial flow because the inertia and buoyancy force on the particles will retard their motion. Nevertheless, the mere existence of flow along the arc, regardless of its speed, rules out any porosity of the arc as long as the gas densities are in the continuum range.

Further and more detailed evidence that the arc column is impervious to the external flow is found in the measurements of Roman[5] and Roman and Myers[6,7], which also show flow separation near the maximum section of the arc, and a near stagnant wake. They find from spectrograph studies that, though the external fluid was air, the radiation from the arc was practically pure argon, which was injected at the cathode to inhibit oxidation of the electrode.

These results indicate that the internal flow in the arc column is from cathode to anode in the Roman-Myers subsonic investigations but from anode to cathode in the supersonic experiments reported here. The cathode jet will exist in both instances but in the supersonic flow the steady arc is slanted with the anode upstream so that a strong fluid pressure gradient along the arc exists, causing flow along the column toward the cathode; the downstream enlargement of the arc near the cathode in Fig. 3 is probably the region where the two streams converge and leave the arc. In the subsonic flow the arc is normal to the stream so that no axial pressure gradient is generated.

Other interesting features of the photographs are (1) the curling of the arc around the cathode and (2) the sharp upstream boundaries. The curling

around the cathode is probably caused by the Lorentz force $\vec{j} \times \vec{B}$ acting on the column near the root; as a result the root will move to a position such that the current is parallel to the magnetic field lines. The sharpness of the boundaries was made more striking by comparing photographs made with neutral filters of various intensities; the photographs, given in Ref. 13, show that the upstream boundary does not change perciptibly when the exposure varies by a factor of 10, while the downstream boundary is fixed for an exposure ratio of 3.

3. MEASUREMENTS OF ARC PROPERTIES

The arrangements and circuits for measuring the field properties were practically identical with those used by Bond[2]. They were: arc current and voltage, magnetic field intensity, and the Mach number and stagnation pressure of the airstream. The stagnation temperature was atmospheric throughout; no systematic change in arc properties with changes from summer to winter temperatures were detected. The air was dried before being pumped into the storage tanks and the dew point was kept low enough to avoid condensation effects. These effects were made evident by the difficulty of obtaining steady arcs under high dew point conditions.

Bond's measurements permitted the measurement of only one arc dimension, near frontal or that reflected in the tunnel wall. Measurements of two dimensions were facilitated by simultaneous photographs of two images by means of the arrangement of mirrors shown in Fig. 2. Two views, along and normal to the flow were not possible because of the locations of the external field coils.* The angles were, instead, 16° and 38°, respectively. The balanced arc was oblong with the major axis normal to the cross-flow so that, for a solid elliptical cylinder with the observed eccentricities the error in the measured lateral axis was around 11%. No correction was made

---

*For the Roman-Myers[6,7] subsonic measurements the arc could be balanced along the axis of the field coils; it was thus possible to arrange the mirrors so that the images showed directly the two axes of the arc.

however because, as is shown for instance in Fig. 3, the downstream boundary was less sharp than the upstream and the degree of optical transparency of the arc is not known. Reasons for assuming that the luminous boundaries indicated photographically are near what we may consider the arc boundaries are given in Section 4.

The dimensions of the arc were measured for three Mach numbers, 2.5, 3.0, and 3.5. They are shown in Fig. 4. The measurements indicate some inconsistencies, largely because of differences in photographic techniques. The Mach 2.5 measurements are based on high speed Fastax photographs while those at Mach 3.0 and 3.5 were taken at 4 exposures per second with a Nikon camera and 35 mm film. New measurements now underway will use the Nikon camera throughout.

One of the most difficult measurements with the present set-up is that of the electric field strength along the arc. The method used was to take measurements over a range of arc currents with two gaps; if we assume that the cathode and anode voltage jumps do not vary with gap. The field strength will be given by the difference between the two arc voltages. The dispersion of results is large depending primarily on the degree of steadiness of the arc. The results of measurements at the two Mach numbers are given in Fig. 5. It is interesting to note that these results differ little from those measured by Roman and Myers[7] for the subsonic arc.

4. MODEL OF THE BALANCED ARC

The most obvious simplification to provide a basis for comparing the subsonic and supersonic arc is to treat the balanced arc as a two-dimensional cylinder relative to coordinates in the plane normal to the column axis. The conservation equations given in Section 5 would then apply to the results given here for the slanted supersonic arc as well as to those of Roman and Myers[7] for a subsonic arc normal to the flow.

A model of the arc cross-section is in qualitative agreement with observations is shown in Fig. 6. It comprises a core of elliptical shape which is impervious to the external flow and a boundary layer over the upstream boundary through which mass, energy, and momentum are transferred to the external flow. Flow separation at the maximum section is in conformity with the wake traverses of Roman and Myers and with the small wake velocities indicated in Fig. 3.

The internal circulation indicated by the schematic streamlines in Fig. 6 is generated by differential Lorentz forces + $JB\vec{e}_x$ acting upstream on the plasma elements; the phenomenon is conceptually analogous to the generation of convection currents by gravity forces acting on a nonuniformly heated gas contained within a horizontal cylindrical tube. In the arc with constant magnetic field intensity the current density will in general be a maximum along the minor axis shown in the figure and an element with current density greater than that required by a balance between the Lorentz and the pressure

9

forces will be accelerated toward the upstream boundary. The Joule heating J^2/σ in the energy equation (for which there is no counterpart in the convection analogy) causes the temperature and therefore J and JB to increase as an element moves upstream. Thus the effect of the Joule heating will be to intensify the circulation.

The balanced arc will assume a shape such that the fluid pressure in the external flow equals the fluid plus magnetic pressure at the arc boundary. The internal properties become steady when an equilibrium current density or temperature distribution is reached such that the internal circulation and conduction are sufficient for transfer of the heat generated (mainly) to the upstream boundary where the transfer to the external flow takes place through a relatively high temperature gradient.

The apparent dimensions of the arc as given in Fig. 4 will be defined by the isotherm at which the intensity of the radiation in the visible range is sufficient to expose the photographic film; this temperature threshold is around 5000-6000°K for air, which is also near the threshold above which the electrical conductivity becomes appreciable. Thus, the photographic image defines approximately the cross-section over which the major part of both the Joule heating and the Lorentz body force occur. Exterior to this region the Lorentz force vanishes and the gas is acted on only by pressure and viscous forces. It therefore seems reasonable to assume that the flow a short distance outside the boundary approximates that around a heated solid cylinder with dimensions determined from the photographs.

The internal circulation described above and shown schematically in Fig. 6 is similar to that calculated by Fischer and Uhlenbusch[11] and reproduced in Fig. 7.* Their calculation applies specifically to an arc in a circular tube acted on by a magnetic field as shown. However, considering that the magnetically balanced arc has a core which is impervious to the external flow, the internal circulation shown would still occur but it would be intensified by the pressure gradients and shear stresses in the boundary region. For the balanced arc the external flow would be downward in the figure and the maximum temperature point would be moved toward the upstream boundary.

In the next section this model will be examined in the light of the experimental results and their implications, based on the conservation equations governing flow within the core.

---

*Reference 13 adapts and extends these calculations to show some features of balanced arcs.

5. DISCUSSION OF THEORY AND EXPERIMENTS

Accordingly we consider here the balanced arc column as a two-dimensional cylinder relative to coordinates in the plane normal to the column axis. The conservation equations would then apply to the results given here for a slanted arc in supersonic flow as well as to those by Roman and Myers[7] for an arc oriented normal to a subsonic flow. The considerations will of course be restricted to stations near the midpoint of arc columns with large ratios of length to major lateral dimension. The cylinder is taken as impervious to the external flow. It must however provide for transfer of mass and energy from the arc to the external flow, with the restriction that the rate of mass transfer must be small relative to the rate of mass flow along the column if the two-dimensional flow approximation is to be valid.

The experimental results described later indicate that over the range of arc parameters covered by the supersonic experiments the conservation equations applicable to the arc core can be greatly simplified by assuming incompressible flow and neglecting the effects of radiation, non-equilibrium, self-field, Hall currents; viscous dissipation, and pressure work. The non-dimensional conservation equations can then be written

$$\frac{d\vec{u}}{d\tau} = -\nabla p - \frac{L_c}{Re_1^2} j \, \vec{e}_x + \frac{1}{Re_1} \nabla^2 \vec{u} \tag{1}$$

$$\frac{dS}{d\tau} = \frac{1}{Pr_1 \, Re_1} \nabla^2 S + \frac{EI/\Phi_1}{Pr_1 \, Re_1} j \tag{2}$$

$$\text{div } \vec{u} = \frac{\epsilon \, d}{U_1 \, \rho_1} \tag{3}$$

Following are the meanings of the symbols: $\vec{u} = \vec{V}/U_1$ where $\vec{V}$ is the velocity vector and U_1 is a characteristic speed (evaluated below); $p = P/\rho_1 U_1^2$, where P is the pressure and ρ_1 is a characteristic fluid density; $j = J/J_1$ where J is the electric current density and J_1 is a characteristic current density; $S = \int_{T_b}^{T} k \, dT / \int_{T_b}^{T_1} k \, dT$ is the non-dimensionalized "heat flux potential," where T_b is the temperatures at the arc boundary, T is the local temperature, T_1 is a characteristic temperature, k is the thermal conductivity; E is the voltage gradient along the arc; I is the arc current; ϵ is the source strength required to account for the rate of mass lost at the boundary; ℓ is a characteristic dimension of the arc; $x = X/\ell$, $y = Y/\ell$, $\tau = U_1 t/\ell$ are non-dimensional coordinates and time; $\vec{e}_x$ is the unit vector in the x (upstream) direction. The non-dimensional parameters are L_c, $\rho_1 IB\ell/\mu^2$, where μ_1 is the visoosity coefficient at temperature T_1; $Pr_1 = \mu_1 C_p (T_1 - T_b)/\Phi_1$ where C_{p_1} is the specific heat at temperature; $\Phi_1 = \int_{T_b}^{T_1} C_p \, dT$ is the characteristic heat flux potential; $Re_1 = \rho_1 U_1 \ell/\mu_1$ is the characteristic Reynolds number.

The characteristic current density J_1 is chosen as the total current, I, divided by the area of the ellipse with axes d_x and d_y measured from the photographs. The corresponding electric conductivity $\sigma = J_1/E$ and T_1 is the corresponding temperature. Then ρ_1, μ_1, k_1, C_p, are the values corresponding to T_1. The characteristic length is taken as $\ell = d_y/2$, that is the dimension lateral to the stream. A suitable characteristic velocity U_1 is deduced below from the experimental data.

13

The experimental data indicates that a suitable characteristic velocity is

$$U_1 = \sqrt{\frac{J_1 B d_x}{\bar{\rho}}} \qquad (4)$$

where d_x is the streamwise axis of the arc core. Figure 8 shows that the ratio $U_1/U_{\infty n}$ where $U_{\infty n}$ is the component of the external velocity normal to the arc axis is remarkably independent of the Lorentz parameter at Mach numbers 2.5, 3.0, and 3.5 well as over the range of the subsonic data of Roman and Myers. Physically U_1 is $1/\sqrt{2}$ times the velocity acquired by an element of density ρ_1 while traversing a distance d_x under the sole influence of a Lorentz force $J_1 B$.

From Eq. (4) and

$$L_c = \frac{\rho_1 \, IB \, d_x/2}{\mu_1^2} \qquad (5)$$

it follows that

$$Re_1 = \sqrt{L_c} \qquad (6)$$

Then Eq. (1)-(3) become:

$$\frac{d\vec{u}}{d\tau} = -\nabla p + j\vec{e}_x + \frac{1}{\sqrt{L_c}} \nabla^2 \vec{u} \qquad (7)$$

$$\frac{dS}{d\tau} = \frac{1}{Pr_1 \sqrt{L_c}} \nabla^2 S + \frac{EI/\Phi_1}{Pr_1 \sqrt{L_c}} j \qquad (8)$$

14

Equations (7) and (8) are of the boundary layer type when L_c is large, i.e. the highest order derivatives are multiplied by a small coefficient. Thus, the solutions of (7) and (8) for large L_c will exhibit large gradients.

The parameter L_c, termed the "Lorentz convection parameter," divided by the Reynolds number, Re, is proportional to the ratio of the Lorentz force, J_1B, to the viscous force $\mu U_1/\ell^2$, acting on a representative volume element. As was pointed out in Section 4 an approximate analogy exists between the circulation within the arc generated by the differential Lorentz forces and that generated by differential gravity forces within a horizontal non-uniformly heated cylinder of gas. For the convection phenomenon the Grashof number $\beta g \Delta T \ell^3/\nu^2$ (β is the expansion coefficient of the gas, g is the acceleration of gravity, ΔT is a representative temperature difference) divided by Re, is the ratio of the gravity force to the viscous force acting on a representative element. Thus the analogy may be expressed in terms of the analogous physical meanings of L_c and the Grashof number.

An important difference however, between the arc and the free convection phenomena is indicated by the Joule heating term in Eq. (2). The numerator, EI/Φ_1 is roughly proportional to the ratio of the rate of Joule heating of a representative element, EJ_1, to the net rate at which heat is lost by the element by conduction, k_1T_1/ℓ^2.

$$\text{div } \vec{u} = \frac{\epsilon_d}{\rho_1 U_1} \tag{9}$$

15

Analysis of the experimental results according to the similarity parameters given in Eq. (8) provide a means for determining whether a range of field properties exists over which the simplifications inherent in that equation are justified for at least a first order determination of the internal flow. The plot of Fig. 9 provides these means and, in addition shows the interpolation between the subsonic experiments of Roman and Myers[7] and the supersonic results given here. The subsonic calculations are based on argon, a monatomic gas, while those for the supersonic are based on air. However, use of a boundary temperature of 6000°K avoids much of the variation of the thermal conductivity caused by dissociation of the diatomic molecules in air.

Under these circumstances one sees that the lines for constant current for the supersonic results are remarkably close to being extrapolations of those for the subsonic. Furthermore, one may write approximately

$$\frac{EI}{\Phi_1} = \alpha + \beta \sqrt{L_c} \tag{9}$$

Then, for small L_c, the velocities will be small so that $dS/d\tau$ will be negligible, and Eq. (8) reduces to the Ellenbas-Heller equation, which in its dimensional form is

$$\nabla^2 \Phi + EJ = 0 \tag{10}$$

For large L_c, the conduction term must become small relative to convection and in the limit, the dimensional equation must become

$$\rho \frac{\overline{C}_p}{k} \frac{d\Phi}{dt} = EJ \tag{11}$$

16

where $\overline{C}_p$ and $\overline{k}$ are average values and $\overline{C}_p/\overline{k}$ is assumed constant throughout.

The results indicate that Eq. (7) and (8) are valid first approximations to the conservation laws within the arc over the upper part of the range of L_c for the supersonic arc, the lower limit of applicability being determined by the arc current. At the high values of L_c the internal circulation will be determined largely by the external field intensity. However, as L_c decreases for a given arc current the self field becomes more and more important and the validity of Eq. (8) in which self-field is neglected becomes more and more questionable. Near $L_c = 0$ the arc approaches a circular cross section, since the cross-flow must also approach zero for a balanced arc, and the effect of the self-field on the circulation as well as that of the external field must vanish and we are left with a free-burning arc. Therefore, it is expected that α in Eq. (9) will be a function of the ratio of the self-field to the external field intensity, as well as of the arc current.

An uncertainty in the Roman-Myers investigations stems from aerodynamic interference between the arc and the jet boundaries. Considering the flow about the arc in the same way as that about a solid cylinder of the same dimensions, the "blockage ratio" (the ratio between the projected area of the arc and the cross-section area of the jet) reaches values of around 0.5. Since in wind tunnel tests the blockage ratio is kept under about 0.1 so that the aerodynamic properties of bodies under test will not be appreciably altered by the presence of the stream boundaries, investigation of the effect of the boundaries on the arc properties is advisable. This study will be undertaken as part of the extension of this program.

17

A program currently underway, as part of the Ph. D. dissertation of the third author, is directed toward more detailed and quantitative interpretations of the generalizations shown in Fig. 8 and 9. Refinements of the calculations carried out by the second author toward more realistic representations of the properties of the balanced arc over a wide range of field properties are included in Ref. 13.

6. HEAT TRANSFER AND DRAG

For steady interaction between the velocity, magnetic and thermal fields, the power dissipated per unit length of column, EI, must be transferred to the surroundings. There are basically three modes of energy transfer from the discharge column which are available to balance the power dissipated. These are radiation, mass transfer and forced convection. Near the roots, energy transfer to the electrodes is also available.

With certain qualifications, comparison with experimental data of heat transfer from solid cylinders is useful. The curve empirically determined by numerous independent experimental investigations on heated cylinders in transverse flow, commonly referred to as Hilpert's curve, is restricted to relatively small differences in temperature between the cylinders and the free stream. A close comparison of the present data with that of solid cylinders, thus, is limited to an order of magnitude considerations. While a close comparison of arc Nusselt number with solid cylinder data is not justified, nevertheless, it remains that if the arc has a boundary layer type structure between the internal and external flow fields, then Nusselt numbers within an order of magnitude would be expected. Hilpert presents his empirical results for circular cylinders perpendicular to the free stream in the form

$$Nu = m(Re_f)^n \qquad (12)$$

where Nu is the Nusselt number and Re_f is the Reynolds number based upon film properties. The coefficients m and n are known for temperature differences up to about $1000^O C$. With different values for m and n Hilpert's relationship also holds for cylinders with non-circular cross sections when the diameter of the circular tube of equal exposed surface is used as the characteristic length. The effect of slant upon heated wires are assumed to carry over to the slanted arc column.

The Nusselt numbers of the discharge column were calculated in the following manner: First, an average arc temperature was calculated from the average current density and electric field. The properties of air were determined by assuming thermal equilibrium. Neglecting the induced electric field $(\vec{V} \times \vec{B})$ and Hall currents, a scalar conductivity was found, and the associated "average" arc temperature was determined. These average temperatures ranged from $8000\text{-}12,000^O K$. This temperature was used in calculating the Nusselt number because the boundary layer of the column must extend into an isotherm where there is significant electrical conductivity. A linear correction for the slant based was used. The film values for the density, viscosity and heat conduction were computed at the inclined stagnation pressure by averaging over the temperature range up to the average arc temperature. The power generated per unit length of column, EI, is assumed to be transferred to the surroundings entirely by forced convection.

For the subsonic balanced arc, measurements of the power balance showed that a large fraction of the Joule heating, 70%, was transferred to the electrodes and only 4% was transferred to the wake.[5] This power balance is not

expected to carry over to the present supersonic balanced arc for the following reasons: (1) The column area in contact with the electrodes is small compared with the subsonic case. Roman's column at both anode and cathode ends went through water-cooled copper locators which acted as heat sinks. Both the anode and cathode roots were surrounded by metal with the anode striking to coils of water-cooled copper tubing. In contrast, the supersonic arc column was in contact with a heat sink only at the extreme ends and over a much smaller area. (2) Roman's cathode was beneath the anode. He injected argon at the cathode for cooling purposes. Thus, the cathode jet, the argon flow and the buoyancy force were in the same direction, and transferred most of the Joule heating, 55%, to the upper anode region. In the supersonic arc, the anode was beneath the cathode and the interaction of the mass flow along the column from anode toward cathode was in the opposite direction of the cathode jet, causing the column plasma to break out of the arc. The power transferred to the electrodes would thus be smaller for the supersonic than the subsonic balanced arc.

Figure 10 shows the Nusselt number and the ratio of the Joule heating to the power loss by convection as a function of the film Reynolds number.

The Lorentz force acts perpendicular to the column, is of magnitude BI per unit length and, for the steady column, is in the direction to balance the resultant aerodynamic force. A force coefficient based upon the Lorentz force and the velocity component normal to the column is useful because it is analogous to the drag coefficients of both subsonic balanced arc and the solid

cylinder held perpendicular to the free stream. In this manner the interaction of the slanted column with the normal velocity component can be compared with the analogous interactions of other known discharges and solid cylinders.

A normal force coefficient is, therefore, defined:

$$C_N = \frac{BI}{q_\infty \cos^2 \theta_s \, d_f} \tag{13}$$

B is the magnetic field midway between the electrodes and is taken from data reported by Bond[1,2,3]. The slant angle θ_s is based upon the average of many runs and was determined by the strike marks on the anode and cathode. The following values for θ_s taken from Bond's data:

M_∞	$\mu_\infty = \sin^{-1} \dfrac{1}{M_\infty}$	θ_s
2.5	23.6^o	25.6^o
3.5	16.7^o	21.6^o

The term $q_\infty \cos^2 \theta_s$ is the dynamic pressure perpendicular to the column. The reference length d_f is taken from Fig. 4. Computed values of C_N are shown in Fig. 11.

Estimation of C_N or the analogous coefficient for other discharges, particularly those concerned with rail accelerators and circular annular gaps, has yielded variations in the coefficients from 0.33 to 10.1[6].

22

Figure 11 shows that the normal force coefficient is near that for the subsonic arc and for solid cylinders. Based upon this comparison, it is indicated, therefore, that the interaction of the arc column with the free stream is consistent to that of a solid body.

Since the column is slanted, the magnetic field varies along its length. For a discharge at $M_\infty = 2.5$, carrying 300 amperes at a 0.9 in. gap, the force per unit length varies from .139 lbf/in. at the anode to .478 lbf/in. at the cathode. The balancing aerodynamic forces must, therefore, have the same variation.

Precisely how the column achieves the required variation in aerodynamic forces along its length was not determined. It is known from the studies of Bond that the column is a supersonic flow is inclined near the Mach angle of the free stream whether the anode or cathode spot is upstream or the applied magnetic field is uniform in the stream direction[1-4]. Hence, the normal component of the free stream is nearly sonic. Slight variations in angle of attack at near sonic conditions can produce significant changes in the aero- dynamic forces normal to the positive column. In addition, mass transfer from the column can affect the pressure distribution and, hence, the aero- dynamic force can be modified particularly near the region where the anode stream interacts with the cathode jet and breaks out of the column.

7. CONCLUSIONS

1. The balanced arc comprises a core which is impervious to the external flow and a boundary layer through which mass, momentum and energy are transferred to the cross-flow.

2. A characteristic velocity is found for the internal flow, proportional to the cross-flow velocity (with different proportionality factors for subsonic and supersonic cross-velocities) but independent of the Lorentz convection parameter.

3. The plot of EI/Φ_1 versus $\sqrt{L_c}$ provides interpolations between the Roman-Myers results and the supersonic results presented here.

4. Extension of measurements in the subsonic range to higher values of L_c with proper attention to aerodynamic interference at the boundaries will be needed to fix more accurately the interpolation conditions between low and high L_c.

8. ACKNOWLEDGMENT

REFERENCES

1. Bond, C. E., "Magnetic Confinement of an Electric Arc in Transverse Supersonic Flow," AIAA J., Vol. 3, No. 1, January 1965, pp. 142-144.

2. Bond, C. E., "The Magnetic Stabilization of an Electric Arc in Transverse Supersonic Flow," Ph. D. dissertation, 1964, Department of Aerospace Engineering, The University of Michigan.

3. Bond, C. E., "Slanting of a Magnetically Stabilized Electric Arc in Transverse Supersonic Flow," Phys. Fluids J., Vol. 9 , No. 4 , pp. 705, 1966.

4. Bond, C. E. and Potillo, R. W., "Stability and Slanting of the Convective Electric Arc in a Thermionic Rail Accelerator," AIAA J., Reprint No. 67-674.

5. Roman, W. C., "Investigation of Electric Arc Interaction with Aerodynamic and Magnetic Fields," Ph. D. dissertation, 1966, Department of Mechanical Engineering, Ohio State University.

6. Myers, T. W. and Roman, W. C., "Survey of Investigations of Electric Arc Interactions with Magnetic and Aerodynamic Fields," ARL Report 66-0184.

7. Roman, W. C. and Myers, T. W., "Experimental Investigation of an Electric Arc in Transverse Aerodynamic and Magnetic Fields," AIAA J., Vol. 5, No. 11, November 1967, pp. 2011-2017.

8. Thiene, P. G., "Convective Flexure of a Plasma Conductor," Phys. Fluids J., Vol. 6 , No. 9 , pp. 1319, 1963.

9. Lord, W. T., "Some Magneto-Fluid Dynamic Problems Involving Electric Arcs," R. A. E. Report, No. 2909, August 1963.

10. Broadbent, E. G., "A Theoretical Exploration of the Flow about an Electric Arc Transverse to an Airstream using Potential Flow Methods," R. A. E. Report, No. 65056, March 1965.

11. Fischer, E. and Uhlenbusch, J., "D. C. Arcs in Transverse Force Fields," Seventh Symposium on Phenomena in Ionized Gases, 1965.

12. Kuethe, A. M., Harvey, R. L., and Nicolai, L. M., "Model of an Electric Arc Balanced Magnetically in a Gas Flow," AIAA J., Reprint No. 67-96.

13. Harvey, R. L., "An Experimental and Theoretical Investigation of Magnetically Balanced Arcs," Ph. D. dissertation, 1968, Department of Aerospace Engineering, The University of Michigan.
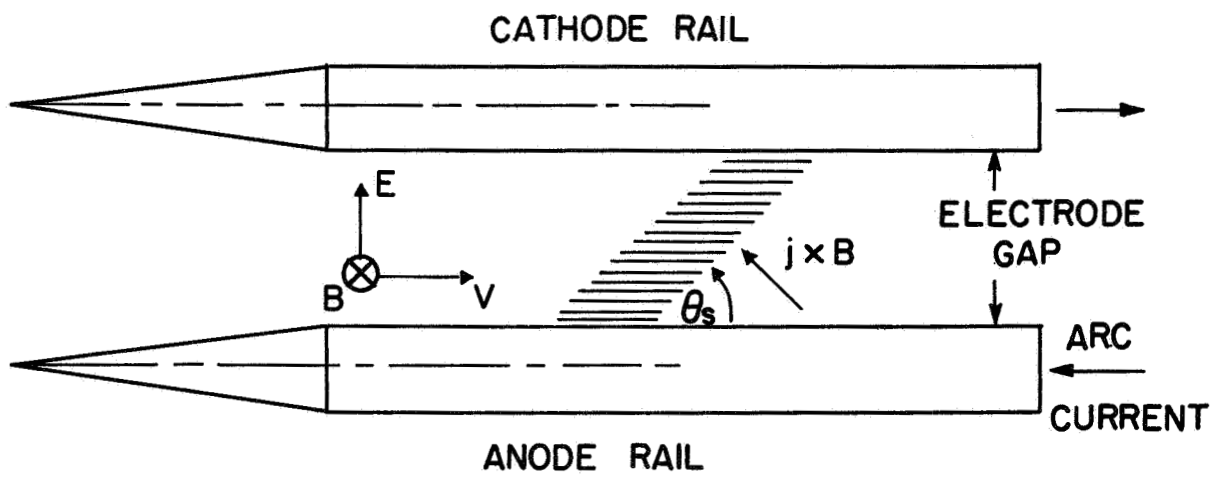
Fig. 1. Orientation of the velocity, magnetic and electric fields.
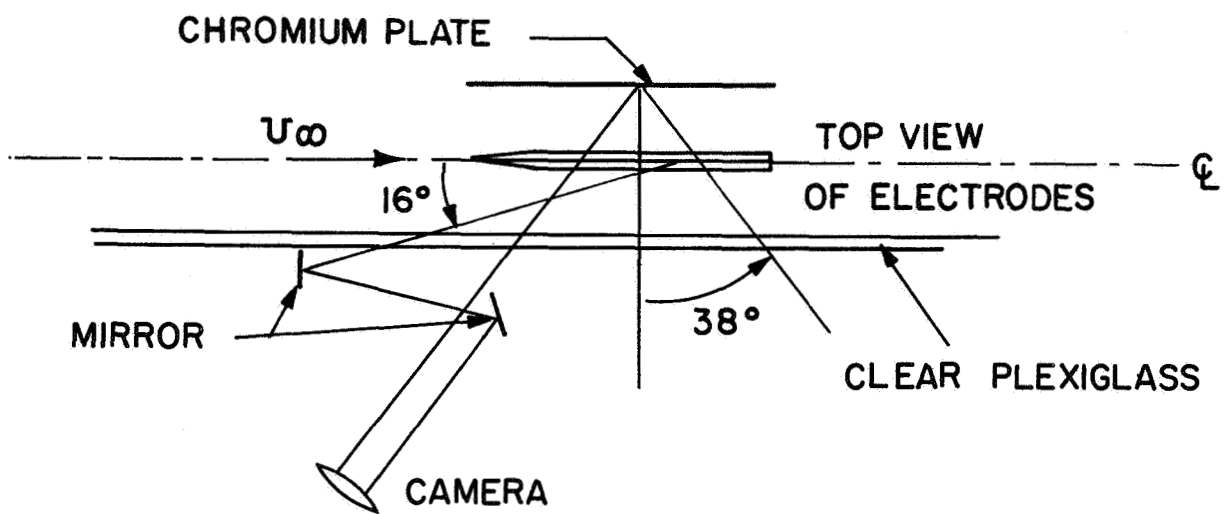
Fig. 2. Mirror and camera arrangement.

1

2

3

4

M_∞ = 2. 5, P_T = 13 IN. HG. , I=300 AMPS.

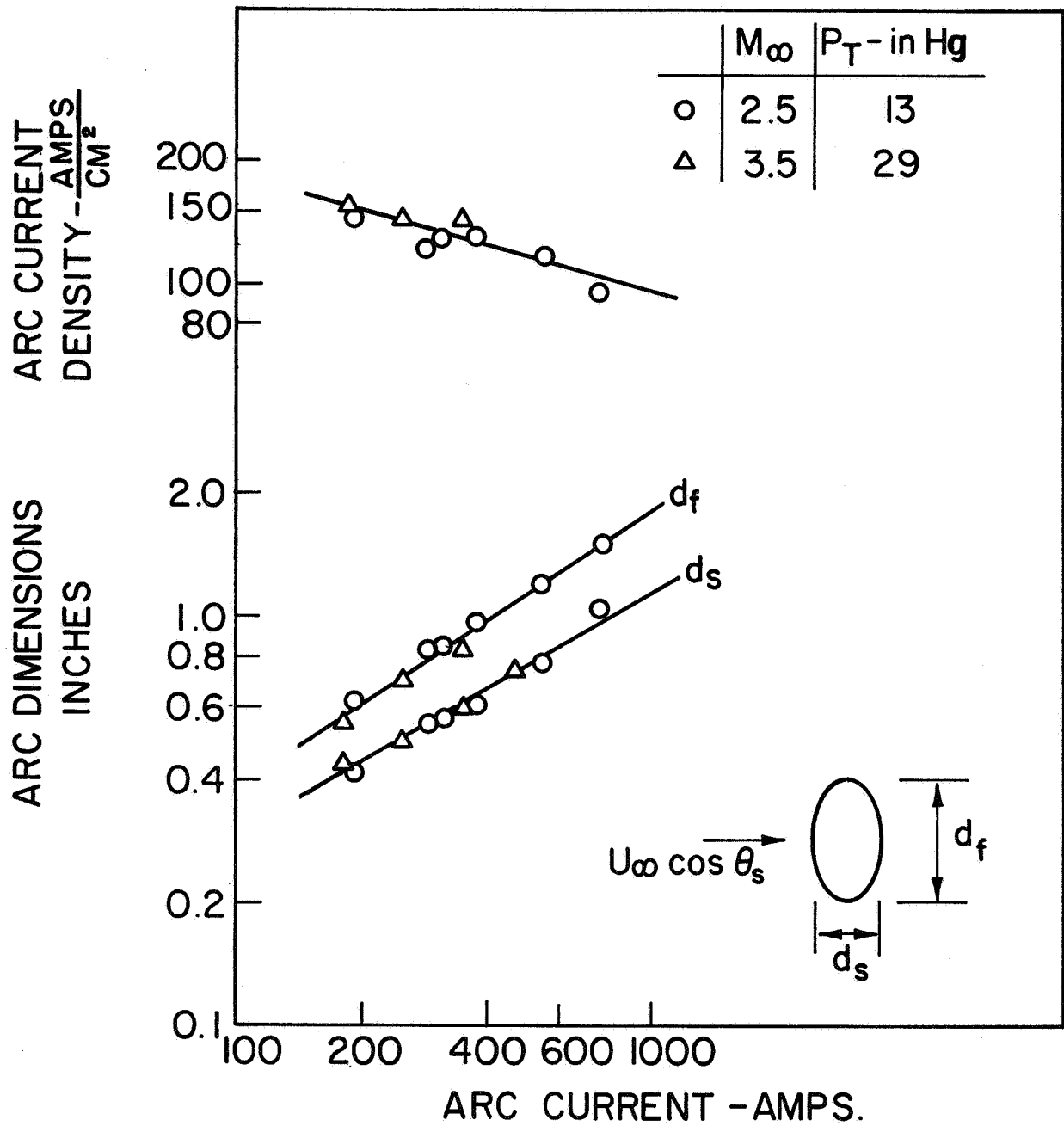ELECTRODE GAP = 0. 9 IN.

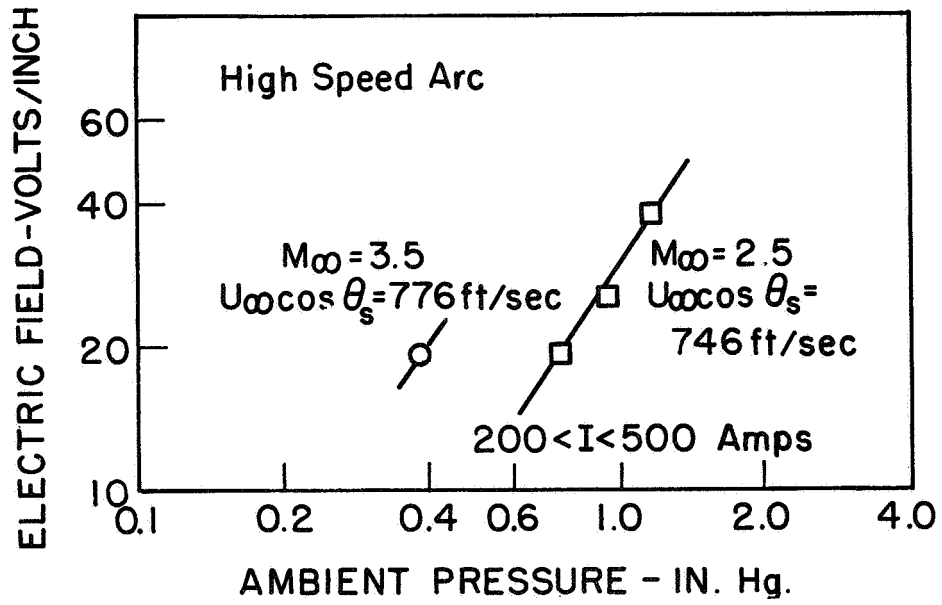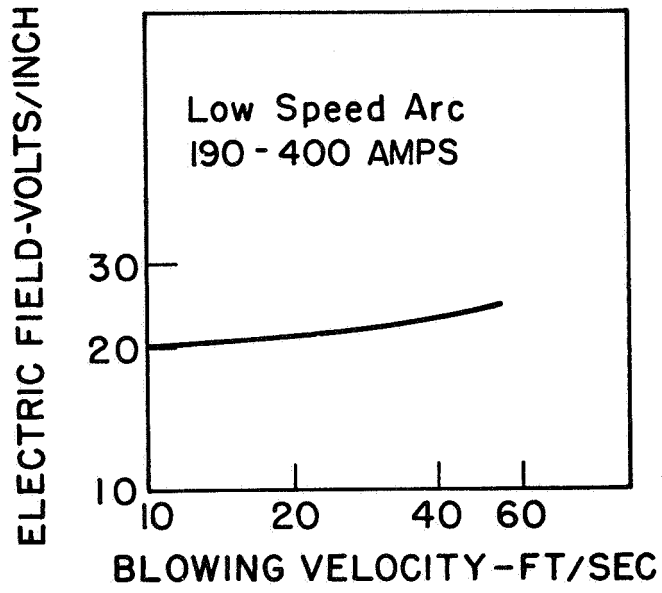Fig. 3. Magnesium tracer particle.

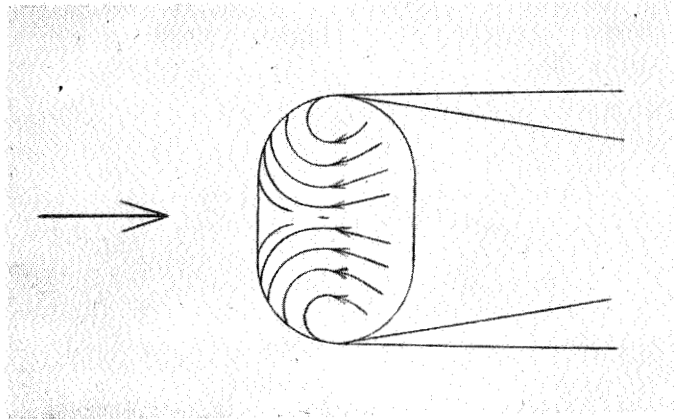Fig. 4. Arc dimensions.

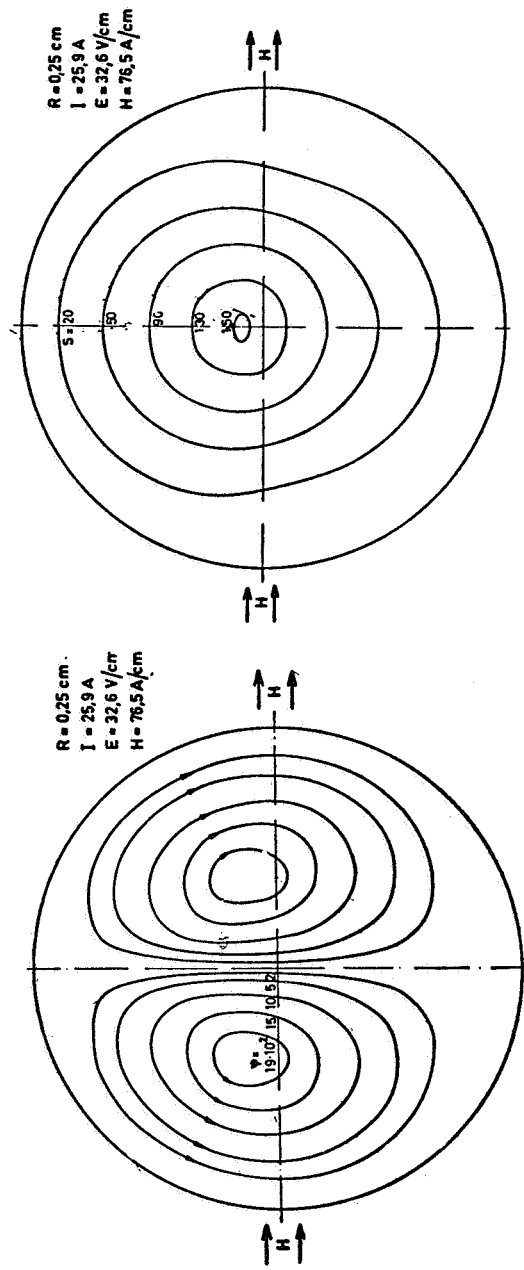Fig. 5. Electric field.

Fig. 6.   Qualitative model of balanced arc.

Fig. 7. Flow field in a constricted nitrogen arc with transverse magnetic field (left). Lines of equal heat flux potential in a constricted nitrogen arc with transverse magnetic field (right).

Fig. 8. Characteristic velocity.

34

$$\dfrac{E\,I}{\displaystyle\int_{6000^{\circ}K}^{T_1} k\,dT}$$

Roman-Myers
Argon Arc in Air
p_{∞} = 760 mm Hg
$.01 < M_{\infty} < .05$

400 amps

300 amps

200 amps

400 amps

300 amps

200 amps

200

M_{∞}	p_{∞} (mm Hg)
▽ 2.5	19.3
△ 3.0	14.5
◯ 3.5	9.6
✕	Interpolated Current Values

$$\sqrt{L} = \sqrt{\dfrac{I\,B\,d_f/2}{\rho\nu^2}}$$
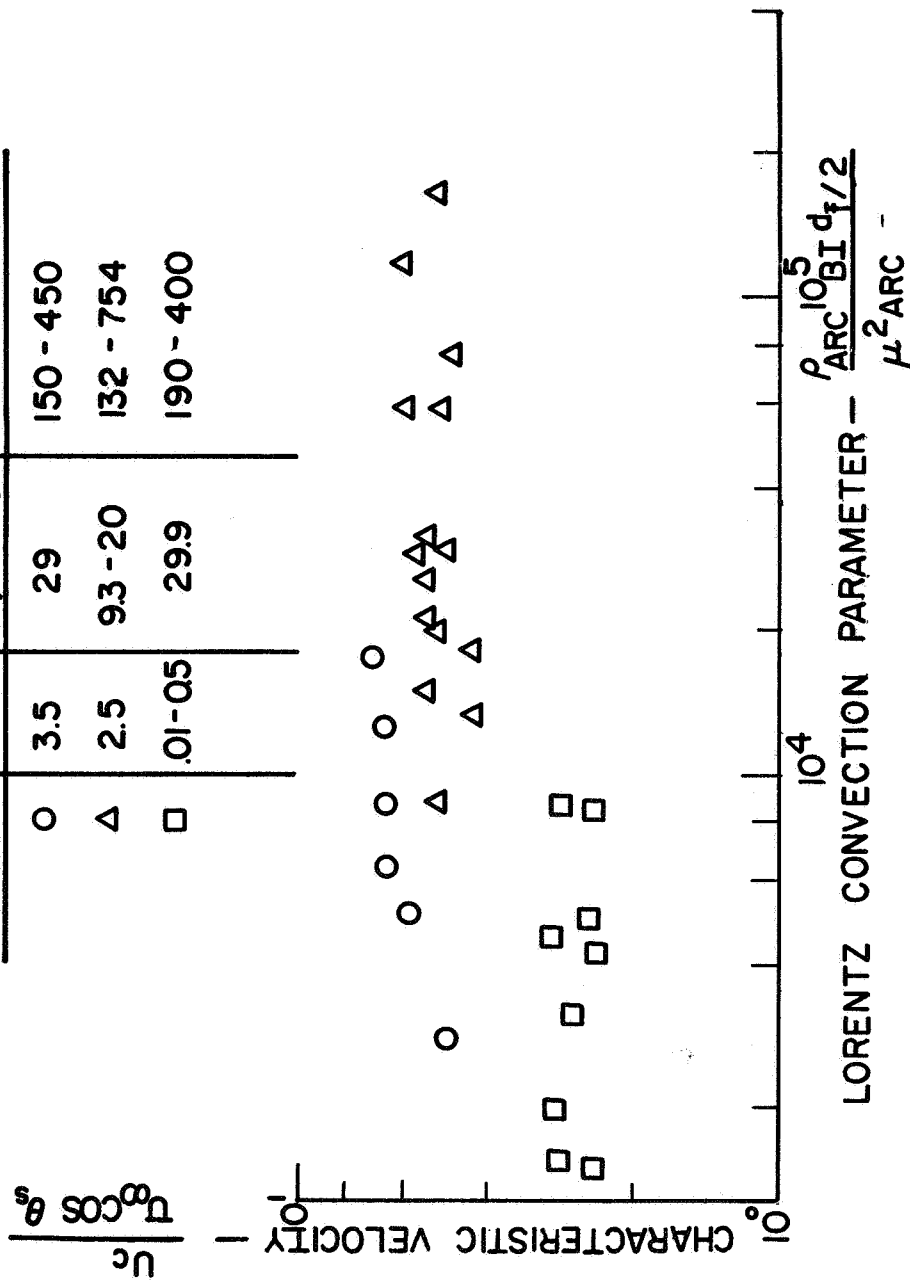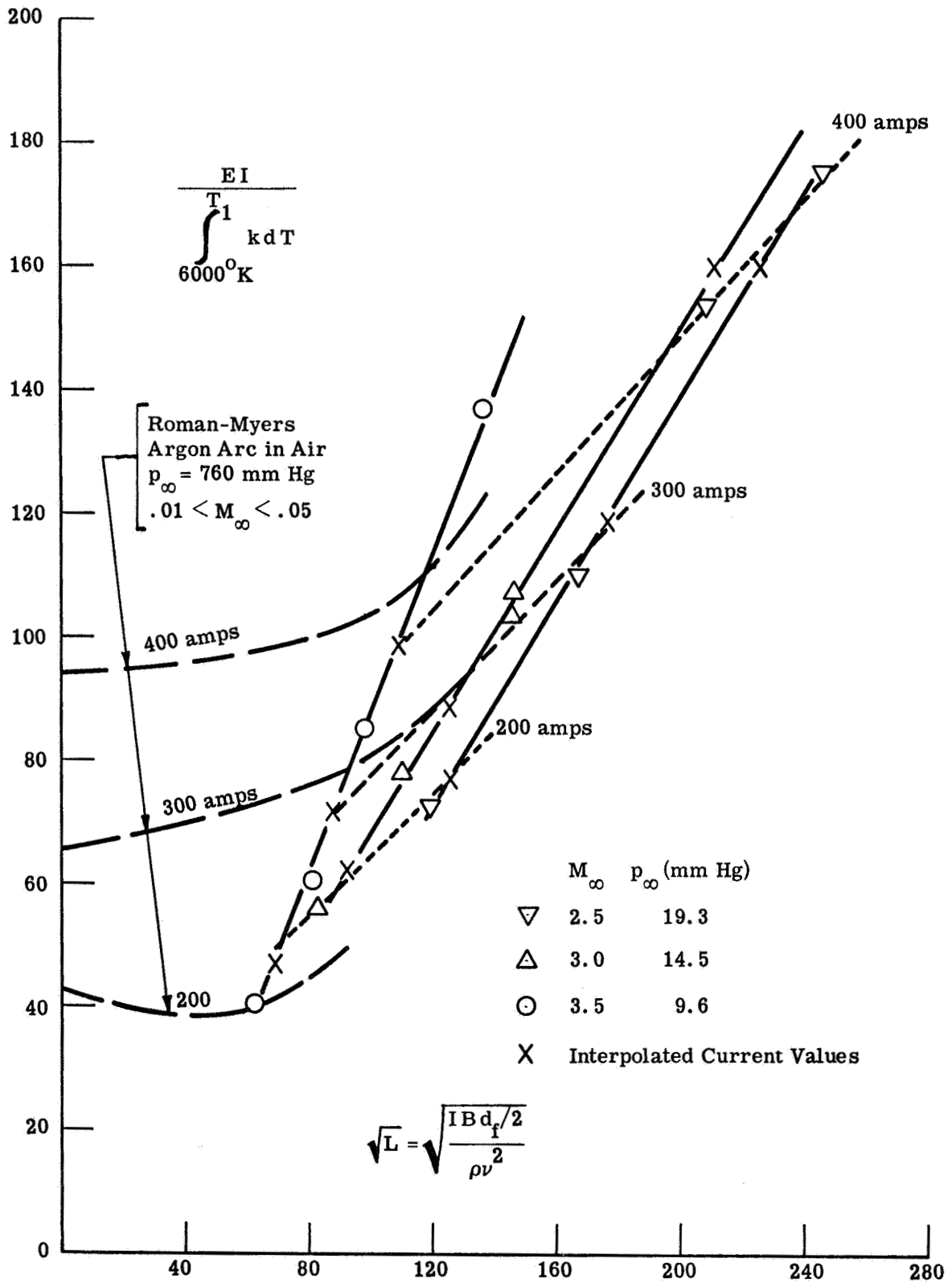
Fig. 9. Power gradient parameter as a function of the
Lorentz convection parameter.
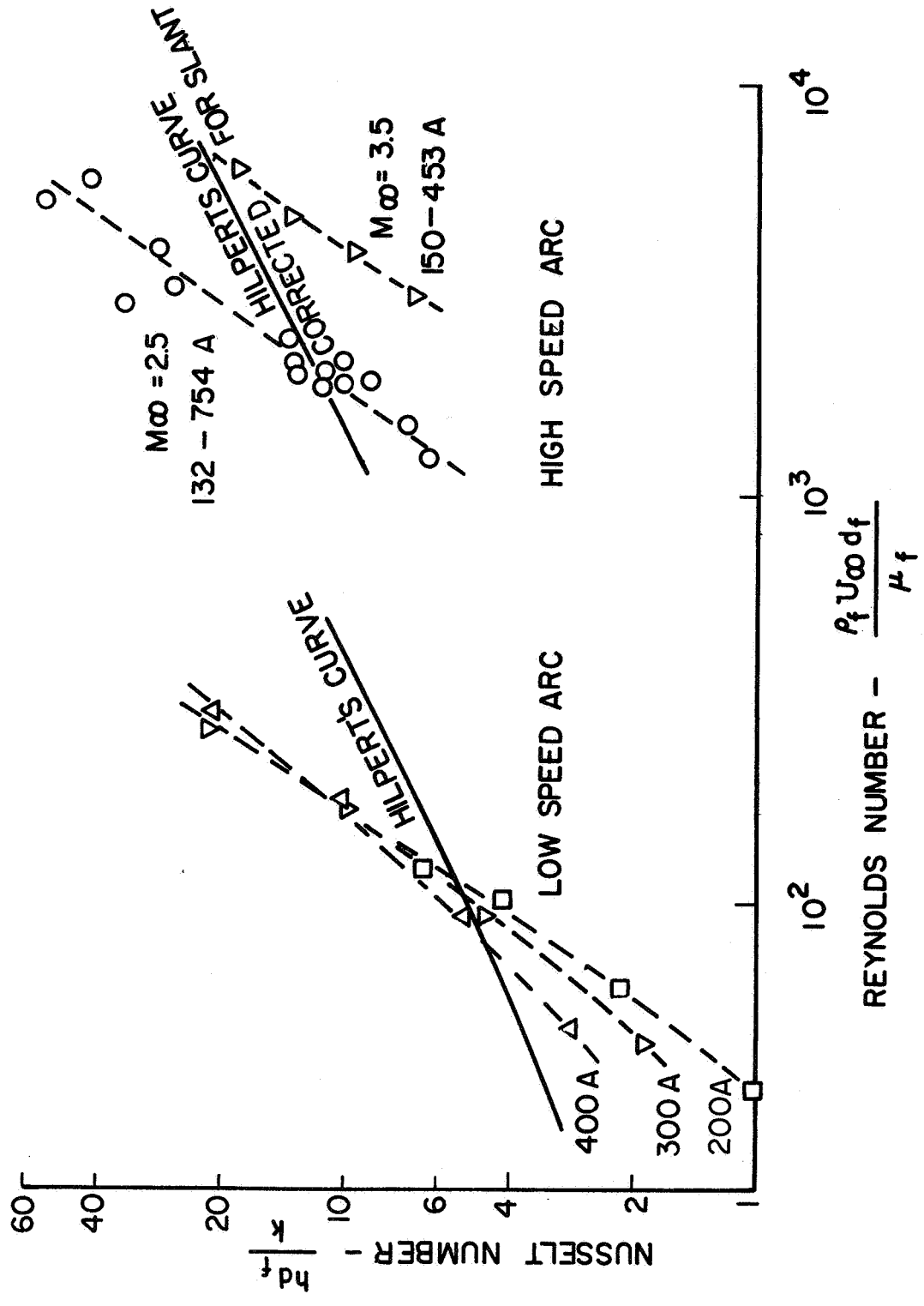
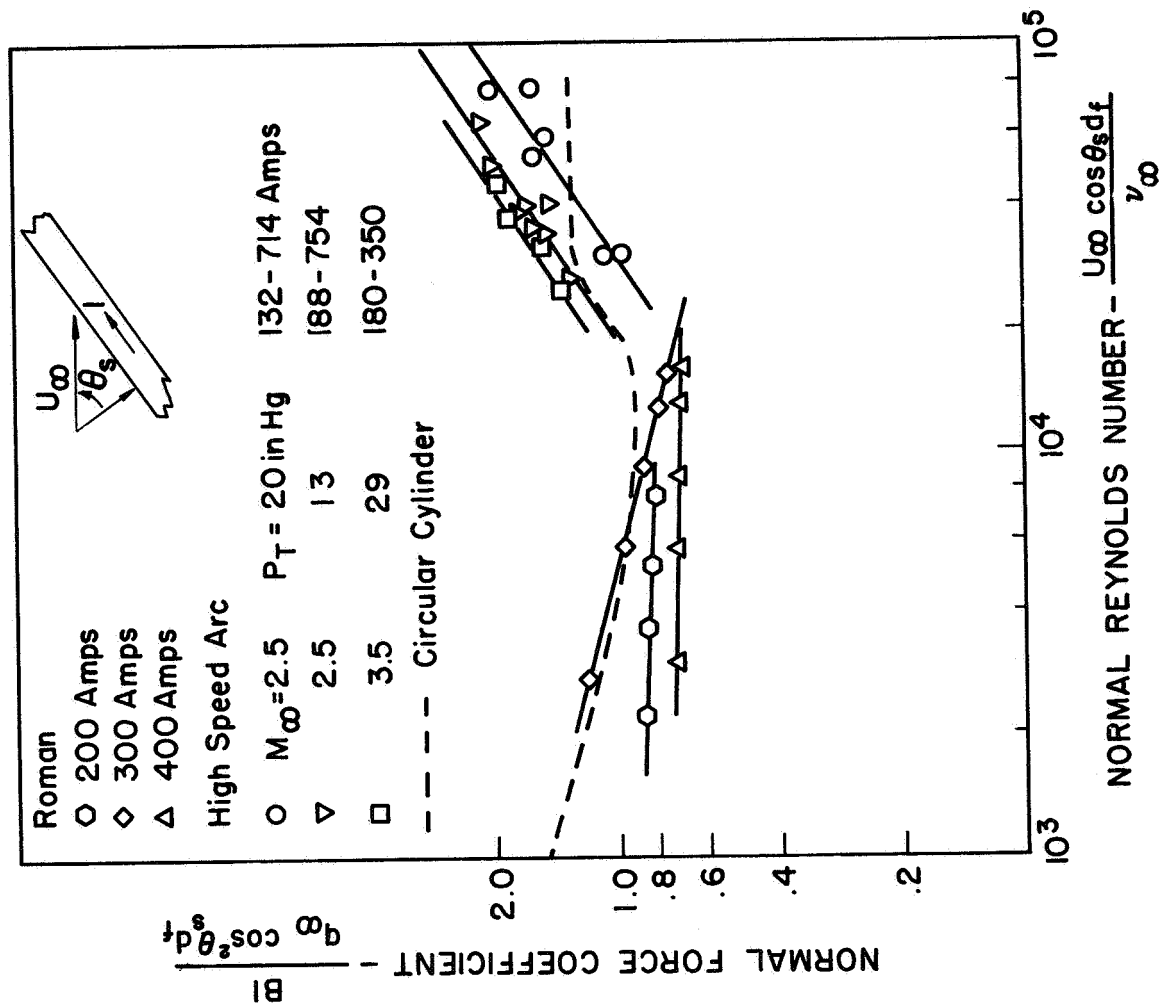Fig. 10. Nusselt number versus Reynold's number.
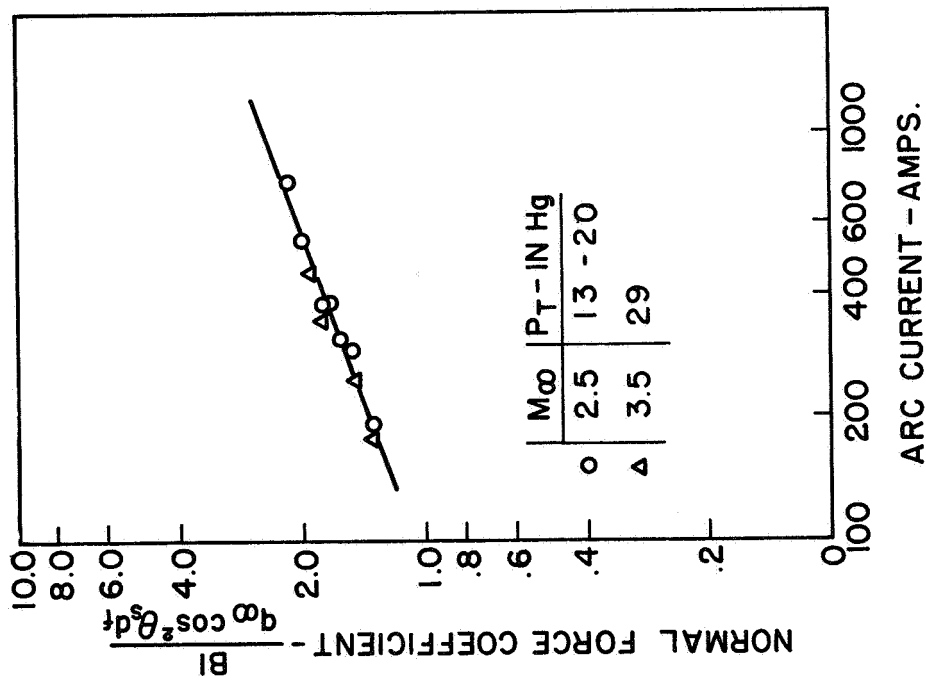
36

Fig. 11b. Variation of normal force coefficient with Reynold's number.

Fig. 11a. Normal force coefficient.

37